Cumhuriyet Science Journal
e-ISSN: 2587-246X
ISSN: 2587-2680
Cumhuriyet Sci. J., 41(2) (2020) 527-533
http://dx.doi.org/10.17776/csj.661666

Power analysis of robotic medical drill with different control approaches

***Yunis TORUN*[1,*] *Sefa MALATYALI*[1]**

[1]*Department of Electrical and Electronics Engineering, ROBOLAB, Faculty of Engineering, Sivas Cumhuriyet University, Sivas/ TURKEY*

Abstract

Increasing the efficiency of the systems used in surgical operations has become an important issue. Especially in orthopedic surgery, many surgical systems and instruments are used to reduce the workload of surgeons and increase the success of the operation. Surgical drills, which are one of these systems used in orthopedic surgery, are used in operations such as drilling, cutting and carving in various interventions. Cases such as drill sensitivity and stability are critical to operational success and patient health. In this study, an orthopedic drill design that can be added to a linear motion module or a 6-axis robot manipulator has been realized. Linear Quadratic Regulator (LQR), which is one of the optimal controller methods, Proportional Integral (PI) Controller, which is one of the classical controller methods and Model Predictive Controller (MPC) systems from modern controller systems are designed to perform speed control task of the surgical drill. A drill integrated into the robot manipulator for a constant drilling speed of 120 rad/sec and a robot manipulator were used to provide constant feed rate (1 mm/s) and to drill holes at constant intervals during the drilling experiments. Power analysis is performed in real-time in bone drilling operations for three controllers. Current, and voltage information during drilling are recorded simultaneously in the experimental setup. In particular, it has been observed that the power signal and the force information of the bone in different layers are proportional.

Article info

History:
Received: 19.12.2019
Accepted: 17.04.2020
Keywords: Bone Drilling, Robotic Surgery, Power Analysis.

1. Introduction

Bone drilling operations are widely used in the treatment of fractured bones in orthopedic surgery [1-3]. Since it is not possible to intervene with broken plaster for the treatment of broken or shattered bones, screw holes are drilled through surgical drills to fix the nails placed in the bone and treat bone fracture [4]. High sensitivity and stability in bone drilling are crucial to both patient health and surgical success [5,6]. In orthopedic surgical bone drilling operations, drill systems have been transformed into wireless (battery-operated) drill systems over time. In these transformation and development processes, there is an increasing demand for features such as more stable, more efficient, more precise working conditions and long-term use of the drills. Features such as sensitivity and stability directly affect operation success and patient health. In order to make a surgical drill system more efficient, power analysis of that drill can be performed with closed loop control for speed control tasks. The power analysis approach is primarily for the power efficiency approach for the long-term and stable operation of the devices. Basic information about power efficiency can be obtained in systems where power analysis is performed [7]. Power efficiency directly affects the operating system and performance of the drill. The power irregularity of a surgical drill used in bone drilling procedures in orthopedic surgery may cause the surgical drill to lose some function or to malfunction. This risk may not only shorten device life but also compromise patient health during surgery.

In orthopedic surgery, bones that are pierced and fixed with nails and screws in bone drilling operations consist of three basic bone layers [8]. These layers are the first cortical bone in which the perforation starts, the spongy bone and the second cortical bone layer in which the perforation is terminated [9,10]. These bone layers have different mechanical properties. Due to these differences, the obtained current and voltage signals during the drilling process also change. Based on the change in these quantities, power analysis can be performed.

*Corresponding author. *Email address:* ytorun@cumhuriyet.edu.tr
 ©2020 Faculty of Science, Sivas Cumhuriyet University

As a result of the literature research, no studies have been found regarding the power analysis of surgical drills. Only Deng et al., have designed a Fuzzy Force Controller for the vertebral laminated milling process, used the power consumption information to ensure the safety of the operation. They calculated the power consumed by each milling layer by separating the motion in the bone as transverse and longitude motion. They have identified three different situations where power consumption differed by looking at the structure of the bone and they have developed the safety controller according to the stop point of milling [11]. However, drill power optimization with different control approaches has not been developed yet in any study up to our best of knowledge in literature.

In this study, power analyzes of surgical drill used in orthopedic surgical operations are performed. The electrical and mechanical model of the motor of the drill has been extracted. Linear Quadratic Regulator (LQR) which is one of the optimal control methods, Proportional Integral (PI) Controller which is one of the classical controller methods and Model Predictive Controller (MPC) systems from modern controller systems have been applied in real-time. On the bone prototype, which mimics the mechanical properties of the sheep femur, 10 holes are drilled for each bone in equal spacing with constant feed rate and constant rotation speeds. During drilling experiments, power analysis can be performed by taking instant current and voltage. The average power values consumed by the drill during the drilling experiments have calculated using different methods.

In Section II, bone layers and drilling path information, the used drill direct current motor model in the study and controller designs for the power analysis are given. Section III provides information on the experimental setup and equipment to which the study is carried out. The results of the experiments are given in Section IV. Finally, Section V concludes the current research.

2. Material and Methods

In bone drilling operations in orthopedic surgery, the amount of power consumed by the drill varies in different layers of bone. The power consumed when the drill is idle is equal to the amount of power required to rotate the drill. When the drill is in the first and second cortical tissues, the amount of power consumed due to the mechanical properties of the bone is maximum. In order to monitor and analyze these power changes during the drilling process, firstly the mechanical properties of the bone tissue to be used in the drilling experiments and the drilling path expressing the direction of the drill bit's progression are mentioned. Then, the design of the motor model of the direct current motor to be used in drilling experiments and the design of the proposed controller systems for power analysis in orthopedic surgical drills have implemented.

2.1. Bone layers and drilling path

The bone structure, which is fixed and treated with nails and screws, generally consists of 3 basic bone layers in orthopedic surgery [8]. These bone layers consist of the first cortical bone, spongy bone and the second cortical bone layer [9], [10]. Depending on the type of surgical procedure performed, bone drilling is divided into two steps. These are the perforation process between the two cortical bones (the perforation of the bone from the opposite wall) and the perforation of only one cortical bone (without necessarily passing through the medullary canal) [12], [13]. When the mechanical elastic properties of the bone are examined, the elasticity of an average age human bone is approximately 17 GigaPascal (GPa) in length and 12 GPa in width. The elasticity of cancellous bone is 0.1-4.5 GPa depending on bone density [14]. Furthermore, because of its structure, the cortical bone layer exhibits more strength than the cancellous bone layer [15]. In Figure 1, the bone layers in the orthopedic surgical bone drilling processes and the drilling path, which represent the direction of progress of the drill bit, are given.

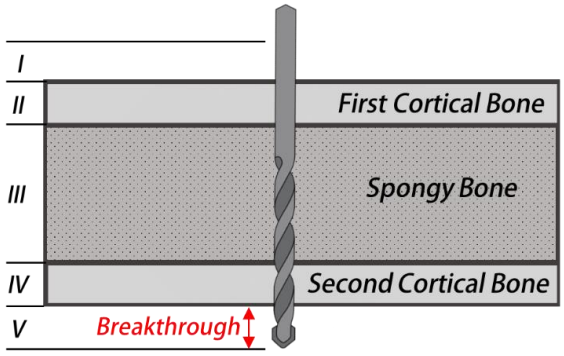

Figure 1: Bone layers and drilling path

Here, the drill does not work before drilling in zone I. Also, the drill does not work after drilling in zone V. Zone II shows the First Cortical Bone layer, where drilling starts. Zone III shows the spongy bone in which drilling is performed. Zone IV refers to the Second Cortical Bone layer. Zone V refers to the breakthrough of the drill bit from the second

cortical layer of the femur bone. The feed distance of the drill bit in Zone V shows the feed distance of the drill bit in tissues such as vessels, nerves, muscles or tendons.

2.2. Direct current (DC) motor model

Direct current motors are widely used in many sectors, especially in industrial applications [16]. It is widely used because the production process is easy and cost-effective. The DC motor mathematical model is less complex than other motor models. This facilitates the formation of the speed/position controller system of the motor is used. Figure 2 shows a model of a direct current motor.

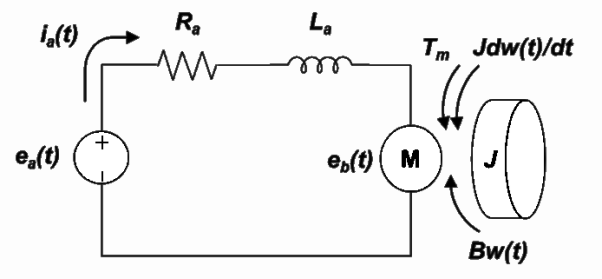

Figure 2: Direct current motor model

In accordance with the above direct current motor model, the electrical parameters of the motor are expressed in Equation 1 as;

$$e_a(t) = i_a(t).R_a + L_a.\frac{di_a(t)}{dt} + e_b(t) \quad (1)$$

, where e_a is the input voltage, R_a is the motor ohmic resistance, L_a is the motor inductive reluctance, e_b is the counter-electromotive force and i_a is the motor current. DC motor counter electromotive force is given in Equation 2.

$$e_b(t) = K_b.w(t) \quad (2)$$

K_b is the constant of the counter electromotive force and $w(t)$ is the angular velocity (rad/s). The relation of the electrical model and mechanical model is expressed in Equation 3.

$$T_m(t) = K_m.i_a(t) \quad (3)$$

$T_m(t)$ is the shaft rotor torque. DC motor mechanical model is given in Equation 4.

$$T_m(t) = B.w(t) + J.\frac{dw(t)}{dt} + T_L(t) \quad (4)$$

B is the motor friction, J is the rotor inertia and T_L is the load torque. State-space representations of the DC motor are Equation 5 and Equation 6.

$$\begin{bmatrix}\dot{w}(t)\\ i_a(t)\end{bmatrix} = \begin{bmatrix}-\frac{B}{J} & \frac{K_m}{J}\\ -\frac{K_b}{L} & -\frac{R}{L}\end{bmatrix}\begin{bmatrix}w(t)\\ i_a(t)\end{bmatrix} + \begin{bmatrix}0\\ \frac{1}{L}\end{bmatrix}.e_a(t) \quad (5)$$

$$w(t) = [1 \quad 0]\begin{bmatrix}w(t)\\ i_a(t)\end{bmatrix} \quad (6)$$

The motor used is a geared motor and the total system inertia and friction coefficient vary in the motor model. Total friction and inertia values in the system in Equation 7 and Equation 8, respectively:

$$B_t = B + B_r red^2 \quad (7)$$

$$J_t = J + J_r red^2 \quad (8)$$

is expressed as. Here, red is the ratio of the gearbox. In the motor used in bone drilling processes, the ratio of the reducer is constant and *red=1/16*. Parameters of used DC motor previously estimated in our previous work with Nonlinear Least Estimator and Genetic Algorithm.

2.3. Controller methodologies

In this study, Linear Quadratic Regulator (LQR), Proportional-Integral (PI) Controller and Model Predictive Controller (MPC) controller methods, which are frequently used among the controller systems, are used. Although PI control is widely used in many control tasks because of its cost-effective, there are some disadvantages as fine-tuning, wind-up. LQR is another approach to improve the controller performance. However, it needs to know the mathematical model of the physical system and the states of the physical system must measurable. MPC provides to the limitation of controlled signals with predicting the response of the system. In this section, the controller methods used in the study, are LQR, PID, MPC are given.

2.3.1. Linear quadratic regulator (LQR)

The Linear Quadratic Regulator Controller method is a control method based on the Optimal Controller Theory and uses the change of states as feedback [17]. Using this method, the feedback vector can be calculated without manipulation of the poles. The operating system of the LQR controller is based on a minimization of the cost function. Figure 3 is a simple diagram of the LQR controller for the DC motor.

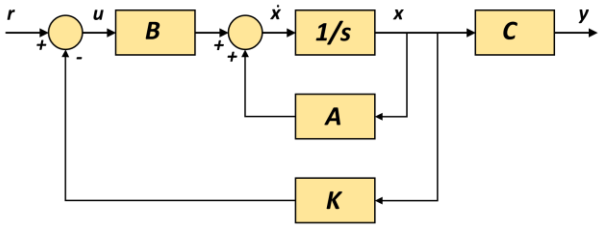

Figure 3: Block diagram of LQR

The K state feedback vector is given in Equation 9 as;

$$u(t) = -Kx(t) \quad (9)$$

where u(t) is the control signal, x (t) is the state of the model. Since LQR is a model-based control method, it calculates the K feedback control coefficient according to the optimal control theory using model state equation coefficients.

In the study, R=1 and $Q = \begin{bmatrix} 9400 & 0 \\ 0 & 40 \end{bmatrix}$ were selected and $K = [87.128 \quad -16.283]$ was calculated.

2.3.2. Proportional integral (PI) controller

It is an easy-to-implement closed-loop controller method that enables to control the system using the proportional and integral sums of the PI error signal [18], [19]. Also, a basic PI Controller block diagram is given in Figure 4 in which K_p is the coefficient of proportional and K_i is the coefficient of integral. The error signal is the *e(t)* represents the difference between the given reference input and the model output. PI minimizes system errors with closed-loop and the system can react to disturbing effects.

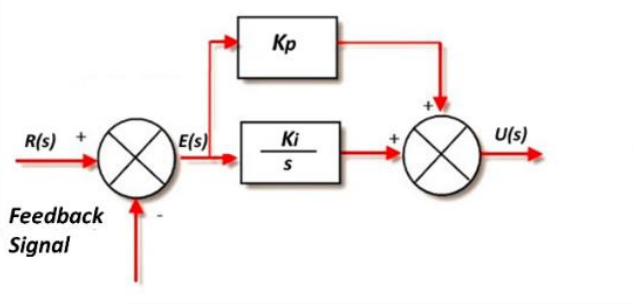

Figure 4: Block diagram of PID

The control parameters Kp = 0,128 and Ki = 0,773 were determined with MATLAB PID Tuner Toolbox for the PI control system.

2.3.3. Model predictive controller (MPC)

Model Predictive Controller (MPC) is a controller method designed according to the system model to be audited. MPC is a highly successful and advanced controller method in many applications [20]. The MPC calculates the optimal controller signal according to the optimization criterion based on the input and output information and the limits set in the past and present. MPC calculates the future behavior of the system with the control signal to be applied to the system. The Floating Horizon Method is used to generate the controller signal. In this method, the first value of the controller signal calculated at each step is applied to the system [21]. Figure 5 graphically describes the steps and operating principle of a single output and single input system with MPC.

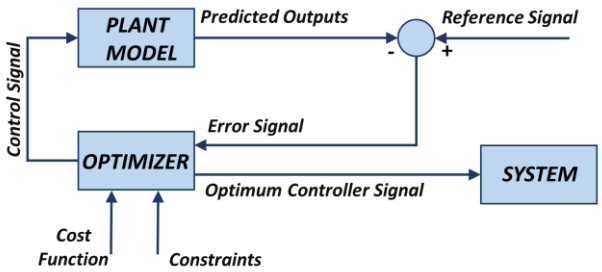

Figure 5: Block diagram of MPC

3. Experimental Setup

In the study, an 18V DC motor was used to provide the torque and rotational movement required for drilling and an encoder was used to measure the rotational speed. In the study, an 18V DC motor was used for drilling and an encoder was used to measure the rotational speed. The DC motor was used for drilling at a constant drilling speed (120 rad/sec). In addition, the KUKA KR900 robot manipulator, Kuka Robot Language (KRL) was programmed with KUKA Programming to ensure a constant plunge speed (1 mm / s) and a constant drilling distance (10 mm). A medical drill bit with a diameter of 3.5 mm and a length of 70 mm was used for drilling. Data acquisition card was used for real-time data collection and drilling speed control. The card output is insulated to protect the data acquisition card from currents and voltages that could damage the card. A load cell with a measuring range of 0-50 N was used to measure the thrust force. Sheep femur bone was used as drilling material. An Acer Aspire 5750G computer with an Intel® Core ™ i5-2450M CPU @ 2.50Ghz (4 CPUs), 4096MB RAM, and an NVIDIA GeForce 610M graphics card was used to collect data in real-time and to develop and implement DC motor control systems. A drill holder is designed for robot drilling and is produced with a three-dimensional printer. The holder is designed to be mounted on the load cell intended for use. Drill holder parts and assembled states are shown in Figure 6.

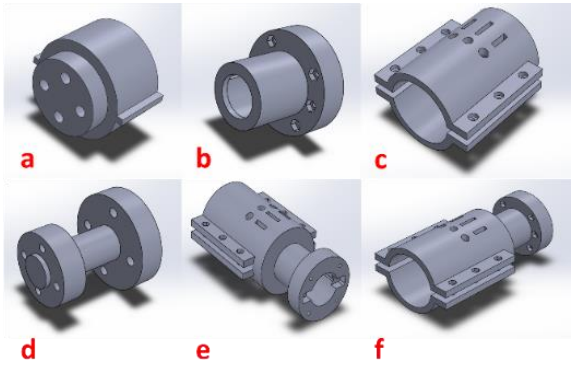

Figure 6: a: Load cell front cover design, b: Load cell outer sheath design, c: Drill motor outer sheath design, d: Load cell and robot attachment design, e: Drill holder design for robot assembled, f: Drill holder design for robot assembled version.

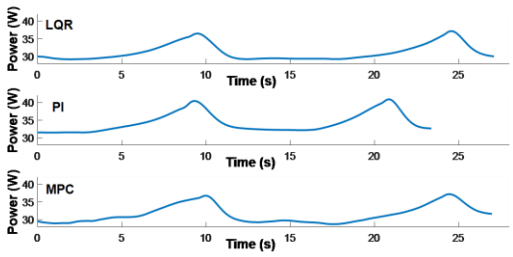

Figure 7: Sheep femur bone with 120 rad / s and 1mm / s Feed Rate

Due to the feature of the bone during drilling, the length of the drilling path is not equal to each other. Therefore, it is necessary to average the power data. The average values of the instantaneous power are given in Table 1.

Table 1: Controller methods for single hole power consumption averages

Controller Methods	Average Consumed Power (W)
LQR	31,2579
MPC	31,5308
PI	34,3473

When the obtained values for instantaneous power are examined, the average power values consumed by the controllers are compared. It is seen that the minimum power consumption is achieved in the drilling experiments performed with the LQR design compared to the drilling tests performed by other methods. MPC power consumption performance was similar to LQR, however, the performance of PI was worse than the other two approaches. Basic

Using the designed drill holder and programmed robot, multiple holes were drilled in the same standard and force, current, voltage, rotation speed and calculated instantaneous power data were collected.

4. Results and Discussions

Bone drilling experiments performed with three controller approaches with drilling 10 holes on sheep femur for each controller. The current and voltage signals were acquired while controlling the drill motor simultaneously. The signals received were also prioritized and examined for the power consumed. The instantaneous power patterns in drilling one hole are shown in Figure 7 with LQR, MPC and PI controller approaches.

Control Voltage, Motor Current and Drill Speed Error signals for LQR control system are given in Figure 8 for a one-hole drilling experiment. Signal waveforms vary according to the stiffness bone being drilled.

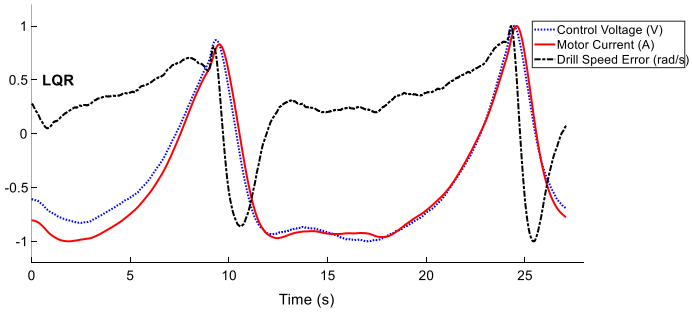

Figure 8: Control voltage (Voltage), motor current (Ampere) and drill speed error (rad/sec) signals for LQR control

5. Conclusion

In this study, an orthopedic drill design that could be adapted to a linear motion module or 6 axis robot manipulators is proposed. Power analyzes of the proposed surgical drill with different controllers were performed. LQR, PI and MPC control approaches were applied to the surgical drill motor in real-time. Power analysis was performed in sheep femur drilling operations in real-time. When performing the power analysis, the current and voltage data during drilling were simultaneously recorded. The result has been analyzed for the instantaneous power analyze based on the current and voltage during the operation of a speed-controlled drill. Improved power analysis accuracy can be improved by further drilling experiments and experiments with human bone.

6. Acknowledgements

This study is financially supported by the Cumhuriyet University Scientific Research Council (CUBAP) with a project number M737. The authors also thank Dr. Özhan Pazarcı for his valuable assistance in bone drilling experiments.

Conflicts of interest

There is no conflict of interest.

References

[1] Dai Y.Xue Y.and Zhang J., Condition monitoring based on sound feature extraction during bone drilling process, *Proceedings of the 33rd Chinese Control Conference*, (2014) 7317–7322.

[2] Chung G.B., Lee S.G., Kim S., Yi B.J., Kim W.K., Oh S.M., Kim Y.S., Park J.and Oh S.H., A robot-assisted surgery system for spinal fusion, *IEEE/RSJ International Conference on Intelligent Robots and Systems, IROS*, (2005) 3744–3750.

[3] Torun Y., Ozturk A., Hatipoglu N.and Oztemur Z., Detection of Bone Excretion with Current Sensor in Robotic Surgery, *UBMK 2018 - 3rd International Conference on Computer Science and Engineering*, (2018) 185-189.

[4] Duan X., Al-Qwbani M., Zeng Y., Zhang W. and Xiang Z., Intramedullary nailing for tibial shaft fractures in adults, Cochrane Database of Systematic Reviews, (2012) CD008241.

[5] Osa T., Abawi C.F., Sugita N., Chikuda H., Sugita S., Tanaka T., Oshima H., Moro T., Tanaka S.and Mitsuishi M., Hand-Held Bone Cutting Tool with Autonomous Penetration Detection for Spinal Surgery, *IEEE/ASME Transactions on Mechatronics*, 20(6) (2015) 3018–3027.

[6] Torun Y., Ozturk A., Aksoz A. and Pazarci O., "Parameters Estimation of Orthopedic Drill," 2019 *27th Signal Processing and Communications Applications Conference (SIU)*, Sivas, Turkey, (2019) 1–4.

[7] Carroll A. and Heiser G., An Analysis of Power Consumption in a Smartphone., *USENIX annual technical conference*, (2010) 271–285.

[8] Torun, Y., Öztürk, A., A New Breakthrough Detection Method for Bone Drilling in Robotic Orthopedic Surgery with Closed-Loop Control Approach., *Ann Biomed Eng.*, 48 (2020) 1218–1229.

[9] Lee W.-Y. and Shih C.-L., Control and breakthrough detection of a three-axis robotic bone drilling system, *Mechatronics*, 2(16) (2006) 73–84.

[10] Farnworth G.H. and Burton J.A., Optimization of Drill Geometry for Orthopaedic Surgery, *Proceedings of the Fifteenth International Machine Tool Design and Research Conference*, (2015) 227–233.

[11] Deng Z., Jin H., Hu Y., He Y., Zhang P., Tian W.and Zhang J., Fuzzy force control and state detection in vertebral lamina milling, *Mechatronics*, 35 (2016) 1–10.

[12] Díaz I., Gil J.J.and Louredo M., Bone drilling methodology and tool based on position measurements, *Computer Methods and Programs in Biomedicine*, 2(112) (2013) 284–292

[13] Mayer M., Lin H.H., Peng Y.H., Lee P.Y.and Wang M.L., A drill signal detection technology for handheld medical drilling device, *Proceedings - 2014 International Symposium on Computer, Consumer and Control*, IS3C 2014, (2014) 958–961.

[14] Turner C.H. and Burr D.B., Basic biomechanical measurements of bone: A tutorial, *Bone*, 4(14) (1993) 595–608.

[15] Zioupos P., Currey J.D., Hamer A.J., The role of collagen in the declining mechanical properties of aging human cortical bone. *J Biomed Mater Res*. 45(2) (1999) 108-116.

[16] Radcliffe P. and Kumar D., Sensorless speed measurement for brushed DC motors, *IET Power Electronics*, 8(11) (2015) 2223–2228.

[17] Farrell M., Jackson J., Nielsen J., Bidstrup C. and McLain T., Error-State LQR Control of a Multirotor UAV, *2019 International Conference on Unmanned Aircraft Systems (ICUAS*), (2019) 704–711.

[18] Nafea M., Ali A.R.M., Baliah J.and Ali M.S.M., Metamodel-based optimization of a PID controller parameters for a coupled-tank system, *Telkomnika (Telecommunication Computing Electronics and Control)*, 16(4) (2018) 1590–1596.

[19] Samin R.E., Jie L.M.and Zawawi M.A., PID implementation of heating tank in mini automation plant using programmable logic controller (PLC), *InECCE 2011 - International*

Conference on Electrical, Control and Computer Engineering, (2011) 515–519.

[20] Bai T.Li S. and Zheng Y., Distributed model predictive control for networked plant-wide systems with neighborhood cooperation, *IEEE/CAA Journal of Automatica Sinica*, 6(1) (2019) 108–117.

[21] Camacho E.F. and Bordons C. (Carlos), Model predictive control, Springer, 2007; pp 14-46.